

Melting of two-dimensional crystals

V. M. Bedanov, G. V. Gadiyak, and Yu. E. Lozovik

Institute of Spectroscopy, Academy of Sciences of the USSR

(Submitted 3 August 1984)

Zh. Eksp. Teor. Fiz. **88**, 1622–1633 (May 1985)

The melting and various characteristics of two-dimensional electron, dipole, and Lennard-Jones systems are studied. The characteristics of a phase transition in a system are discussed as functions of the stiffness of the interaction potential between particles. Molecular-dynamics calculations are carried out over broad ranges of the temperature and the density to find thermodynamic functions, the structure factor, the dielectric function, the translational and orientational correlation functions, the number of disclinations, the velocity and displacement autocorrelation functions, the self-diffusion coefficient, and a modified Lindemann ratio. A two-step picture of the melting, involving the formation of a hexatic intermediate phase, agrees with several results which have been found for a Wigner crystal, on the nonsimultaneous discontinuities in the translational and orientational correlation lengths, the exponent in the orientational correlation function, and the direct observation of topological defects. Data on dipole and Lennard-Jones systems imply a first-order phase transition. The calculations yield a negative sign for the static dielectric function $\epsilon^{-1}(k)$ not only for an electron crystal but also for a comparatively broad region in an electron fluid.

INTRODUCTION

Just how two-dimensional (2D) systems melt has been the subject of a spirited debate (see Ref. 1 and the bibliography there). Although there can be no long-range crystalline order in 2D systems,^{2,3} there may exist phases with different degrees of order, characterized by different asymptotic forms of the translational and orientational correlation functions¹⁾ (Refs. 4–7). A low-temperature phase with a power-law decay of the translational correlation should have a non-zero shear modulus and should support the propagation of transverse sound. In other words, this phase should exhibit properties of a crystal.

Among the questions being debated are the nature of the phase transition and the associated question of the existence of an anisotropic liquid phase (a hexatic phase) as an intermediate step between a crystal and an isotropic liquid. Two possibilities are being discussed:

1. Two-step topological melting.^{5–7} Initially (at a temperature $T = T_1$) dislocation pairs dissociate, and a crystal with a power-law translational order and a long-range orientational order goes into a hexatic phase (with a short-range translational order—an exponentially decaying translational correlation function—and with a power-law orientational order). Later (at $T = T_2 > T_1$) a transition occurs from the hexatic phase to an isotropic liquid as the result of the dissociation of a pair of disclinations. Neither of these transitions causes observable features in thermodynamic quantities.

2. A single first-order transition. Specifically, there is a transition from a crystal (with a power-law translational order) to an isotropic liquid. In this case one should in principle be able to observe discontinuities in the thermodynamic quantities at the point of the transition, the coexistence of two phases, hysteresis, and other effects. The occurrence of a first-order transition may be related to either an instability of the lattice [the vanishing of the shear modulus $\mu(T)$] be-

cause of a phonon anharmonicity below the dislocation dissociation point¹¹ or, for example, a high density of dislocations because of the comparatively small energy of the dislocation core,¹² for which the theory of Refs. 5–7 does not apply.

Either of these scenarios might be valid, depending on the behavior of the shear modulus as a function of the temperature (or as a function of the energy of a dislocation core; in addition to these two scenarios, there might be transitions of various types in various parts of the phase diagram). At the accuracy of the calculations which have been carried out, the temperature at which the phonon anharmonicity causes an instability and the temperature of the dislocation melting agree fairly well with experiments and numerical simulations (more on this below). There is accordingly a need for a more detailed study of the behavior of various structural characteristics as functions of the temperature. Effects caused by substrates and defects greatly complicate experimental efforts to unambiguously resolve the question of the melting mechanism.

An effort has therefore been undertaken to study melting by numerical simulation,¹ where the substrate can be ignored and where there is the unique possibility of extracting all possible physical characteristics of the system—thermodynamic, structural, and kinetic—under known conditions.

In this paper we report studies of three different 2D systems: electron, dipole, and Lennard-Jones systems. We discuss the effect of the stiffness of the interaction potential on melting characteristics.

In our calculations we use a molecular dynamics method to study the behavior of the thermodynamic characteristics, spatial and temporal correlation functions, the static dielectric permeability, and a modified Lindemann ratio. We also analyze lattice defects.

Study of these characteristics shows that the electron

crystal comes closest to the picture of topological melting (§§2,5). The clearest pieces of evidence in favor of this picture are (a) the direct observation of topological defects and their progressive conversion, with increasing temperature, from bound pairs of dislocations into free dislocations (pairs of disclinations) and then into free disclinations and (b) the behavior of the correlation lengths for the translational and orientational correlation functions. Specifically, these correlation lengths begin to decrease sharply at different temperatures: The translational order disappears from the system first, and then the "quasi-long-range" orientational order disappears. In addition, the coefficient η_6 , a measure of the decay of the orientational function [$g_6(r) \sim r^{-\eta_6}$], has a value at $T = T_2$ which is close to the value of 1/4 predicted by the theory of topological melting⁶ ($\eta_6 = 0.26 \pm 0.03$). A different situation, to within the accuracy of our calculations, is found for the dipole crystal (§3) and the Lennard-Jones crystal (§4). The thermodynamic functions jump noticeably, and the translational and orientational correlation lengths decrease sharply, at the same temperature or density, furnishing evidence for a first-order transition in these systems.

Among the rather curious results which have emerged are those resulting from a study of the picture of particle trajectories. It turns out that over a broad region of the liquid phase diffusion occurs preferentially along boundaries between distinct clusters. In the course of this study, another interesting result has been established. The static dielectric function $\epsilon^{-1}(k)$, $k \neq 0$, of a 2D electron system is negative, not only in the crystalline phase but also in a certain region in the liquid phase.

In §1 we discuss our calculation method and the particular characteristics which we calculate. In §2 we report results calculated for an electron system; in §3 and §4 we report results on the dipole system and the Lennard-Jones system, respectively. In §5 the results are compared with the theory of dislocation melting and the theory of melting due to anharmonicity effects. We also discuss the conditions for the occurrence of a topological transitional.

§1. CALCULATION METHOD

For the numerical simulations we use the molecular dynamics method.^{13,14} We place N particles in a rectangular sample with dimensions L_x and L_y , choosing N , L_x , and L_y in such a way that a periodic continuation through the boundaries of the sample does not disrupt the triangular lattice formed by the N particles. In the case of long-range potentials we are forced to choose a square sample (and thus slightly distort the lattice) because of our use of a fast-Fourier-transform algorithm. At the value $N = 504$ which we chose, the distortions amount to less than 2%.

In calculating the forces acting on a particle we cut from the plane a circle of radius r_c centered on the given particle. Binary forces are taken into account exactly inside this circle.

Long-range effects are important for the Coulomb and dipole systems, so we use a method which is a combination of a particle-particle method and a particle-grid method.¹⁵ All other particles outside the circle r_c and also the periodic

transforms of all of the particles are incorporated through a solution of the Poisson equation by fast Fourier transforms.

For the Lennard-Jones system, we find corrections to the pressure and to the interaction energy from the assumption that the particles are distributed in a radially symmetric way. We use a link-list algorithm¹⁵ to rapidly search for and find the particles.

In our calculations for the Lennard-Jones system we use $r_c = 2.4\sigma$, where σ is the parameter in the Lennard-Jones potential, $\Phi_{L-J}(r) = 4\epsilon((\sigma/r)^{12} - (\sigma/r)^6)$; this choice is equivalent to incorporating the first three coordination spheres. For Coulomb and dipole systems we use $r_c = 5.6a$, where a is the "ion" radius, $a = 1/(\pi n)^{1/2}$, and n is the density. The classical equations of motion are solved by a temporally second-order accurate method. The time step is chosen in such a way that the total energy of the system is conserved within $\sim 0.05\%$ over the calculation time.

The calculations for any of the systems begin with the crystalline phase. The particles are placed at the sites of a regular lattice, and small displacements are specified by a random-number generator. The system then relaxes to the given temperature. This relaxation continues for several thousand time steps. A switch to a different temperature is made by scaling the velocities; then the system relaxes freely to equilibrium. A switch to a different density is made in two stages: first the coordinates are scaled and then the velocities are adjusted to the necessary temperature.

In addition to calculating the thermodynamic properties (the temperature, the pressure, the internal energy, and the specific heat) we calculate density correlation functions: the translational correlation function

$$g_G(R) = \langle \rho_G(0) \rho_G^*(\mathbf{R}) \rangle, \quad \rho_G(\mathbf{R}) = \exp(i\mathbf{G}\mathbf{u}(\mathbf{R})), \quad (1)$$

where $\mathbf{u}(\mathbf{R})$ is the displacement of a particle from site \mathbf{R} , and \mathbf{G} is a reciprocal-lattice vector; and the orientational correlation function

$$g_6(r) = \langle \psi(0) \psi^*(\mathbf{r}) \rangle / g(r), \quad (2)$$

$$\psi(\mathbf{r}) = \frac{1}{N} \sum_{j=1}^N \frac{1}{n_j} \sum_{k=1}^{n_j} \exp(i\theta_{kj}) \delta(\mathbf{r} - \mathbf{r}_j),$$

where n_j is the coordination number of the j th particle, θ_{kj} is the angle between some fixed axis and the vector \mathbf{r}_{kj} , which connects nearest neighbors, and $g(r)$ is the radial distribution function. The structure factor is calculated by a numerical integration from the expression

$$S(k) = 1 + 2\pi n \int_0^\infty dr (g(r) - 1) r J_0(kr), \quad (3)$$

where $J_0(kr)$ is the Bessel function. The static dielectric function $\epsilon^{-1}(k)$ is calculated in terms of $S(k)$.

The temporal correlation functions, i.e., the autocorrelation functions for the velocity,

$$Z(t) = \langle \mathbf{v}(0) \mathbf{v}(t) \rangle / \langle |\mathbf{v}(0)|^2 \rangle, \quad (4)$$

and for the displacement,

$$\chi(t) = \langle |\mathbf{r}(0) - \mathbf{r}(t)|^2 \rangle / 4t, \quad (5)$$

are averaged over the N particles and also over the initial times (over a random sample of 60 time points).

The self-diffusion coefficient is calculated in two ways: by integration of the velocity autocorrelation function,

$$D_1 = \langle |\mathbf{v}|^2 \rangle \int_0^\infty Z(t) dt, \quad (6)$$

and from the Einstein formula

$$D_2 = \lim_{t \rightarrow \infty} \chi(t). \quad (7)$$

In the calculation of the correlation lengths and the exponents for the power-law decay we study the decay of the correlation functions $g_G(R)$ and $g_\delta(r)$ at large distances by finding a fit with simple functions of the type

$$f_1(r) = A \exp(-r/\xi), \quad f_2(r) = Br^{-\eta}. \quad (8)$$

A transition from one phase to another must be accompanied by a change in the asymptotic behavior, so that there must be changes in the exponent η or the correlation length ξ . From the displacements of the particles from the lattice sites we calculate the modified¹¹ melting parameter

$$\gamma_M = \langle |\mathbf{u}_i - \mathbf{u}_{i+1}|^2 \rangle / a^2,$$

where $\mathbf{u}_i + \mathbf{u}_{i+1}$ is the relative displacement of two neighboring particles (lattice sites in the crystalline phase). The quantity γ_M , in contrast with the Lindemann parameter $\gamma = \langle u^2 \rangle / a^2$, does not diverge in an infinite 2D system, so that it can serve as a phenomenological melting parameter. Indeed, the values of γ_M turn out to be nearly independent of the nature of the 2D crystal according to the theory of melting due to phonon anharmonicities¹¹ and according to our numerical calculations (as discussed below).

§2. COULOMB SYSTEM

The classical Coulomb system is characterized by the dimensionless parameter

$$\Gamma = e^2 / akT, \quad a = 1 / (\pi n)^{1/2}, \quad (9)$$

where n is the 2D density.

Figure 1 shows the calculated behavior of the internal energy of the system, $U = U(T)$. The behavior changes significantly at $\Gamma = 145-159$. By calculating the fluctuations of T or taking the derivative $\partial U / \partial T$, we can calculate the specific heat. The calculations yield $C = 1.81k_B N$ at $T < T_1$ (the crystal) and $C = 1.57k_B N$ at $T > T_2$. As the temperature is raised further, the specific heat falls off, but only very slightly.

The reason the specific heat has approximately the same values in the crystalline and liquid phases lies in the persistence of the (dynamic) cluster structure well into the

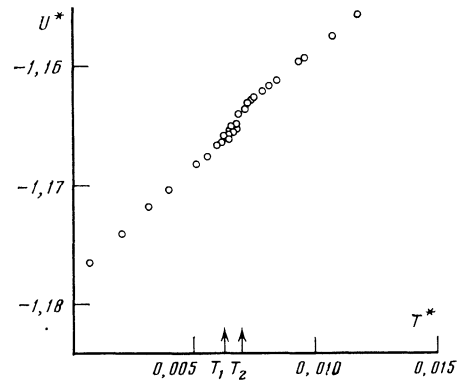


FIG. 1. The internal energy per particle versus the temperature $T^* = 1/\Gamma$ for a 2D Coulomb system. The energy is expressed in units of $e^2 a$, where $a = (\pi n)^{-1/2}$.

liquid phase.¹⁴ Most of the particles are in clusters and are oscillating near their equilibrium positions; only a few of the particles move between clusters.

There are two ways to reproduce the crystalline phase. First, the initial state of the system can be specified as a random sprinkling of the particles over a square. In this case a slow "cooling" of the system to large values of Γ leads to a triangular equilibrium lattice. However, dislocations, interstitials, and other defects arise in the system in the course of such calculations; in other words, the system goes into a metastable state, from which it cannot escape, at least during the calculation time. Accordingly, for an adequate reproduction of the crystalline phase we specify at the outset an ideal lattice with small random displacements (§1). When we take this approach we observe, after the relaxation of the system, only quartets of disclinations (pairs of dislocations with opposite Burgers vectors) in the crystalline phase.

Figure 2 shows the growth of disclinations with the temperature. Calculations of the number of disclinations by two algorithms yield approximately the same results.¹⁶ These involve (1) calculating the number of disclinations from the number of nearest neighbors which lie within a circle of radius R_0 [$R_0 \approx (R_1 + R_2)/2$, where R_1 and R_2 are the radii of the first and second coordination spheres] and (2) calculating the number of disclinations from the number of vertices in Voronoi polygons. We accordingly used the first

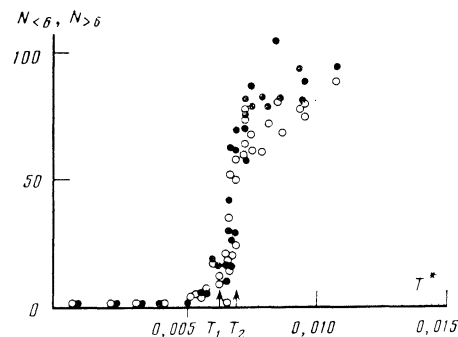


FIG. 2. Increase in the number of disclinations with the temperature. Coulomb system. ●—negative disclinations, $N_{>6}$; ○—positive disclinations, $N_{<6}$.

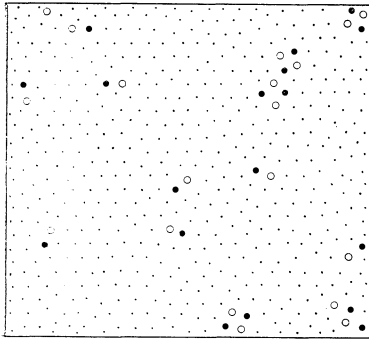


FIG. 3. Some typical snapshots of the particle configurations in the Coulomb system in the transition region. $\Gamma = 149$. Free dislocations can be seen.

and simpler algorithm. More important is the average over the period of the oscillations, which slightly lowers the effective number of disclinations.

Before the beginning of the phase transition there is an insignificant concentration of disclinations in the crystalline phase, ~ 0.02 . After the phase transition at T_1 , this concentration changes to ~ 0.2 . In the intermediate region, $T_1 < T < T_2$, dissociated dislocation pairs appear (Fig. 3), and ultimately free disclinations appear.

We have also calculated the translational correlation functions (1) for several values of Γ near the phase transition. In the crystal ($\Gamma > 159$, $T < T_1$) the translational correlations decay only slightly and propagate out to the middle of the calculation cell (≈ 30 coordination spheres). The exponent η_G increases with the temperature, having the value $\eta_G = 0.14$ at $\Gamma = 189$, for example. At $\Gamma < 159$ the translational correlations decay in accordance with $\exp(-r/\xi)$ ($\xi = 1.4a$ at $\Gamma = 149$).

We carried out calculations of the orientational correlation function $g_6(r)$ for various of Γ . In the crystalline phase, the function $g_6(r)$ approaches a constant value $g_6(L/2)$ at large distances (Fig. 4); this constant value decreases as the liquid phase is approached. A correlation is also retained in the orientation in the intermediate region, $T_1 < T < T_2$, while

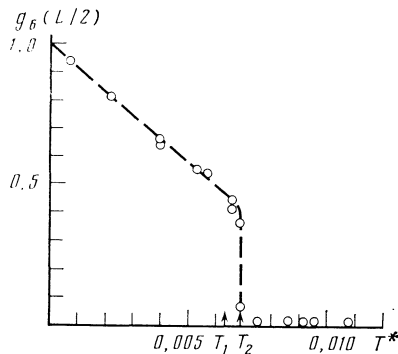


FIG. 4. "Asymptotic behavior" of the orientational function for a Coulomb system. The approach to a nonzero constant value and the slow decay to zero on the interval $T_1 < T < T_2$ cannot be distinguished because the dimensions of the sample are too small. $T^* = 1/\Gamma$.

it fades away (begins to fall off exponentially over distance) at temperatures $T > T_2$. In the interval $T_1 < T < T_2$, approximating $g_6(r)$ by the function $f_2(r) = Br^{-\eta_6}$ leads to an exponent $\eta_6 \lesssim 0.26$, which reaches a maximum value at $T = T_2$.

That the order disappears at different times in the orientation and the translation can be seen in Fig. 5, which shows the behavior of the corresponding correlation lengths. Note that the dimensions of our system make it possible to follow the transition from a power-law decay to an exponential decay (the jumps in Fig. 5), although it is not possible to reliably distinguish a power-law decay with a small exponent from the approach to a nonvanishing constant value in the case of the orientational correlation function. There is accordingly a temperature interval $T_1 < T < T_2$ (corresponding to the interval $145 < \Gamma < 159$) in which the orientational order persists, but there is no translational order. The melting region found here agrees with the results of actual experiments on electrons at the surface of liquid helium.¹⁷

Calculations of the radial distribution function $g(r)$ and of the structure factor $S(\mathbf{k})$ show that the heights of the peaks decrease, while their widths increase, with increasing T . At very high temperatures, $\Gamma \approx 1$, the peaks disappear, and the structure factor becomes a monotonic function of the wave vector. In the latter case, $S(\mathbf{k})$ agrees with the Debye-Hückel approximation.

The modified melting parameter¹¹ γ_M increases almost linearly with increasing T . Near the melting temperature, T_1 , the increase in $\gamma_M(T)$ becomes sharper, and at the point $T = T_2$ there is an abrupt increase in γ_M . At T_2 we have the value $\gamma_M(T_2) \approx 0.1$. Qualitatively the same behavior is observed for $\gamma_M(T)$ for the dipole system and the Lennard-Jones system. The critical values of $\gamma_M(T_2)$ for those systems are again ~ 0.1 ; i.e., $\gamma_M(T)$ is a nearly universal parameter.

From the calculated structure factor we calculated the dielectric function $\epsilon^{-1}(\mathbf{k}, \omega = 0)$ (Fig. 6). It follows from these calculations that the dielectric function is negative, $\epsilon^{-1}(\mathbf{k}) < 0$, over a rather broad range of the parameter Γ , including the liquid phase. In this range of Γ , there are some quite distinguishable clusters. It might thus be suggested that the negative sign of ϵ^{-1} here is associated with the short-range crystalline order. With increasing Γ in the liquid phase, a maximum appears in $\epsilon^{-1}(\mathbf{k})$; this maximum approaches zero at $ka \approx 4.5$, signalling the proximity of the

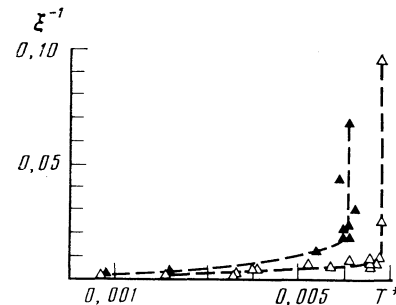


FIG. 5. Reciprocal correlation lengths (in units of a^{-1}). \blacktriangle —Translational; \triangle —orientational. The sharp increase is evidence of the vanishing of the corresponding order parameters. Here $T^* = 1/\Gamma$.

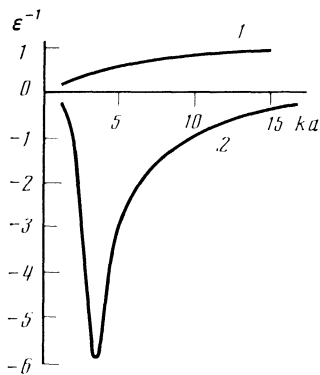


FIG. 6. Static dielectric constant. Coulomb system. Γ : 1—1; 2—10. The quantity $\epsilon^{-1}(k)$ becomes positive everywhere and a monotonic function of the wave vector when the spatial correlations disappear from the system.

point of the transition to the crystalline phase. These results on ϵ^{-1} agree with the analyses by Kirzhnits and by Dolgov and Maksimov.¹⁸

Our calculations of the autocorrelation functions for the velocity and the displacement illustrate the changes in the kinetic properties of a Coulomb system at the various values of Γ . The velocity autocorrelation function oscillates at a characteristic frequency $\omega_m \approx 1.2\tau^{-1}(\tau = (ma^3/e^2)^{1/2})$; the damping of the oscillations becomes more pronounced as the temperature is raised, but the frequency ω_m does not change. The displacement autocorrelation function $\chi(t)$ has three characteristic regions (Fig. 7): 1) a linear region, with a slope which increases with the temperature; 2) a transition region with several oscillations; and 3) the onset of saturation in the liquid phase (the onset of a diffusive regime) or a decay in the crystalline phase (due to the finite particle oscillation amplitude). The time over which saturation sets in is determined by the characteristic "free-flight" times, which are determined by short-range correlations in the system.

§3. DIPOLE SYSTEM

Let us examine a classical 2D system of parallel dipoles. Such a system is characterized by the dimensionless parameter Γ_d , given by

$$\Gamma_d = D^2/2kT a^3 \quad (10)$$

(D is the dipole moment). In a dipole system, in contrast with a Coulomb system, there is no need to introduce a compen-

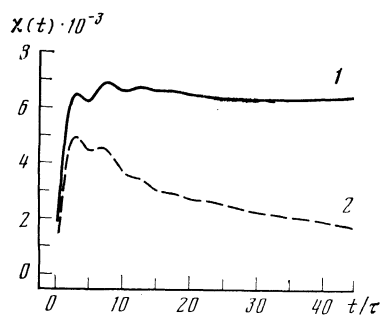


FIG. 7. The displacement function. Coulomb system. Γ : 1—144; 2—184.

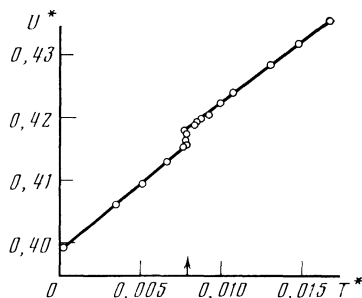


FIG. 8. The internal energy per particle as a function of the temperature $T^* = 1/2\Gamma$. Dipole system (the energy is expressed in units of $D^2/2a^3$).

sating background. In the calculation of the interaction potential energy, the series converge.

The initial energy of a dipole system has a discontinuity (Fig. 8) of $0.16kT_m$ per particle at the melting point, $\Gamma_d = 62 \pm 3$. Also jumping sharply at the point of the phase transition is the amplitude of the first maximum of the structure factor. The correlation lengths calculated from observations of the damping of the oscillations of the radial function $g(r)$ and of the orientational function have structural features at a common temperature (Fig. 9).

§4. LENNARD-JONES SYSTEM

The search for the hexatic phase and the analysis of the properties of the Lennard-Jones system were carried out for the $T^* = 1.0$ isotherm and for the isochore $n^* = 0.8$ ($T^* = kT/\epsilon$, $n^* = n\sigma^2$).

4.1 Isochoric ensemble. The system goes through several phases as it moves along an isochore. We have identified the following phases: a phase in which a gas and crystal coexist, at $0 < T^* < 0.37$; a phase in which a liquid and a crystal coexist, at $0.42 < T^* < 0.69$; and a liquid phase at $T^* > 0.69$.

In the region in which the gas and crystal coexist (low temperatures) the system "collapses" into one of the possible metastable states²⁾ in the course of its evolution; correspondingly, the internal energy is higher and the pressure lower (negative).

These states are associated with the presence of an energy barrier for the formation of a vacancy in the interior or at the surface. We have calculated the average interparticle dis-

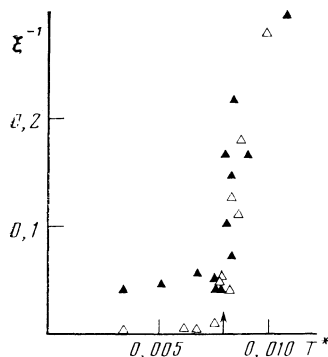


FIG. 9. Reciprocal correlation lengths. Dipole system. \blacktriangle —Translational; \triangle —orientational. Within the errors, the two order parameters disappear simultaneously (cf. Fig. 5).

tance as a function of the temperature, finding it by systematically processing all pairs of nearest neighbors. In one of the metastable states (the “stretched crystal”), the average distance between particles is slightly greater than in a crystal with pores. Below the temperature $T^* \approx 0.27$, the average distance d/σ does not change, while in an ideal crystal this distance would have to decrease to $d/\sigma = 2^{1/6} \approx 1.1225$, corresponding to the lowest potential energy of the interparticle interaction. This value can be found by extrapolating the calculated data from the interval $0.27 < T^* < 0.4$ into the interval $0 < T^* < 0.27$.

A correlation analysis of this system leads to a temperature dependence of the correlation functions which is qualitatively the same as that for a Coulomb system.

The orientational order (Fig. 10) is retained in all the phases, including the coexistence phases, disappearing only in the liquid phase.

Analysis of the autocorrelation functions of the velocity, $Z(t)$, suggests a fundamental distinction between a system with a short-range interaction potential and systems with a long-range interaction. The function $Z(t)$ exhibits a quite rapid asymptotic decay. Only for the low-temperature phase do we see several oscillations. The autocorrelation functions for the displacements are of the same nature as in Fig. 7.

A calculation of the self-diffusion coefficient from expressions (6) and (7) reveals good agreement.

4.2 Isothermal system. The calculation of an isotherm begins in the crystalline phase ($n^* = 0.94$). The pressure has a characteristic van der Waals loop with a metastable region ($\partial p/\partial n < 0$) in which two phases coexist: a crystal and a liquid. Away from the phase transition, small systems reproduce quite well the results derived with a large number of particles. Near the phase transition, the depth of the metastable state depends on the dimensions of the system (on the number of particles).

In our calculations, the metastable states occupy the interval (along the density scale) $0.88 < n^* < 0.90$. At $0.865 < n^* < 0.88$, a new phase is nucleated, and the old phase is progressively displaced. The disruption of the crystalline order can be seen from the change in the number of those particles in the system which have the correct number of neighbors (Fig. 11). Analysis of topological defects shows that in the crystalline phase there are only quartets of disclinations, while in the transition region we find more complicated defect formations, including free disclinations of

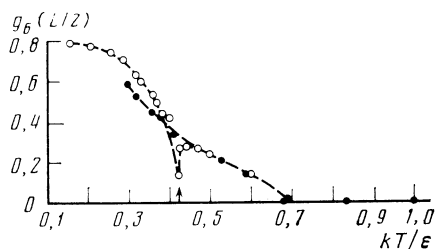


FIG. 10. “Asymptotic behavior” of the orientational correlation function in a Lennard-Jones system. The isochore $n^* = 0.8$. ○—Crystal with pores; ●—“stretched” crystal.

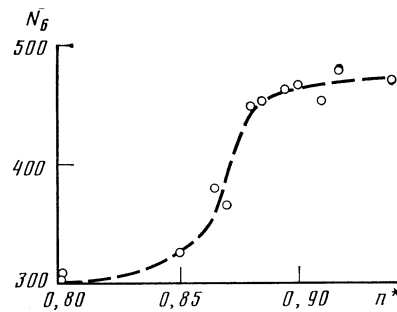


FIG. 11. The number of particles having the correct number of neighbors. Lennard-Jones system. The isotherm $kT/\epsilon = 1$.

both signs. A disclination pile-up creates liquid-phase nucleation regions, which can be seen on our maps of the particle paths as regions of elevated diffusion.

The correlation functions $g_G(R)$ and $g_G(r)$ are similar to those found for the Coulomb system. In a crystal, the translational correlations decay slightly over a distance equal to half the calculation cell and have an exponent $\eta_G = 0.05$ ($n^* = 0.885$). At $n^* = 0.87$, there is a sharp change in the nature of the decay of $g_G(R)$, and a correlation length $\xi \approx 2.6\sigma$ is established. In the liquid phase, $g_G(R)$ decays rapidly over a distance on the order of the first coordination radius ($n^* = 0.85$).

The behavior of the orientational order during the melting is analogous to that of the translational order. This assertion is supported by the behavior of the correlation lengths as functions of the density (Fig. 12). The orientational order and the translational order disappear simultaneously at $n^* \approx 0.87$. At the same density, the $\gamma_M(n^*)$ goes to zero. The critical value of $\gamma_M(n^*)$ is approximately the same as the corresponding values for the Coulomb and dipole systems, and it is about twice as large as in the 3D case.

§5. DISCUSSION OF RESULTS

Let us compare the results on the melting temperature with the theory of a topological transition, actual experimental results, and the theory of melting due to a phonon anharmonicity.

The melting point found above for the electron crystal, $\Gamma = 145$ (cf. Refs. 24–27), agrees well with the experimental value $\Gamma = 137 \pm 15$ found for the melting of an electron

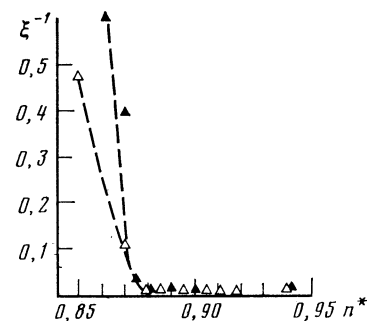


FIG. 12. Reciprocal correlation lengths (in units of σ^{-1}). Δ —Orientational; \blacktriangle —translational. Lennard-Jones system. The isotherm $kT/\epsilon = 1$. Within the errors, the two order parameters disappear simultaneously.

crystal above liquid helium¹⁷ (cf. the results of Refs. 28 and 29). The value $\Gamma_d = 62$ (see also Ref. 30) calculated for a dipole crystal (see Ref. 31) agrees with experiment.

The results found for the melting points also agree well with the results calculated in Ref. 11 for the point in which the lattice loses its stability because of phonon anharmonicities (Lozovik and Farztdinov¹¹ used a version of the self-consistent theory which incorporates skeletal diagrams of order γ_M). The values found in Ref. 11 are $\Gamma = 139.7$ for an electron gas and $\Gamma_d = 55$ for a dipole system. We also note that the critical values of the modified melting parameter $\gamma_M(T_c) = 0.1$ (Ref. 11) are essentially the same as those found in the present study by the molecular dynamics method. It is important to note, however, that near the point where the shear modulus $\mu(T)$ vanishes it changes quite rapidly (because of phonon anharmonicities), so that the solution of the equation $T = \mu(T)/16\pi$, which determines the temperature of dislocation melting for an electron crystal, lies extremely close to the temperature at which $\mu(T)$ vanishes. Another possibility is that this equation has no solutions at all in the region $T < T_0$, where T_0 is the temperature at which $\mu(T)$ vanishes. In this case, there would be no dislocation melting at all. At the accuracy of the calculations of Ref. 11, it is this latter situation which holds for the dipole and Lennard-Jones systems, in qualitative agreement with the results of our own numerical simulations.

The results presented in §§2–4 show that the pictures of the dipole crystal and of the Lennard-Jones crystal are similar in significant ways: At the melting point there are significant jumps in the thermodynamic quantities (e.g., the jumps in the internal energy per particle are $\Delta U \approx 0.20 kT_m$ and $\Delta U \approx 0.16 kT_m$, respectively, for the Lennard-Jones and dipole systems). The orientational order and the translational order disappear at the same point. Furthermore, the melting temperatures agree reasonably well with calculations based on phonon anharmonicities. All these results are evidence of a first-order phase transition.

The results on melting for an electron crystal are apparently evidence of a different picture (§2). Here the behavior of the thermodynamic quantities is smoother. Analysis of topological defects shows that the transition is accompanied by the appearance of free dislocations and free disclinations.

The most important result is that the orientation and the translational order disappear at different temperatures T_1 and T_2 (Fig. 5). This result is a strong argument in favor of the existence of a hexatic phase between T_1 and T_2 . Furthermore, the exponent of the orientational correlation function is found to be $\eta = 0.26 \pm 0.03$ as T_2 is approached, in agreement with the value of $1/4$ predicted by the theory of a topological transition.⁶

We are very indebted to V. L. Ginzburg, L. V. Keldysh, D. A. Kirzhnits, V. L. Pokrovskii, S. M. Stishov, A. A. Chernov, and the participants of seminars led by V. L. Ginzburg

and V. L. Pokrovskii for a useful discussion of these results and for several useful comments.

¹¹Pokrovskii and Talapov⁸ have analyzed the effect of a periodic potential of the substrate, which is of qualitative importance for a commensurate 2D crystal. See Refs. 9 and 10 regarding the effect of substrate defects.

²Our calculations reveal two states of the system at low temperatures: a crystal with pores (calculation A) and a "stretched" crystal (B). Some intermediate states were found in Refs. 19–23.

¹S. K. Sinha (editor), *Ordering in Two Dimensions*, North-Holland, Amsterdam, 1980; R. M. Morf, *Helv. Phys. Acta* **56**, 743 (1983); A. F. Bakker, C. Bruin, and H. J. Hilhorst, *Phys. Rev. Lett.* **52**, 449 (1984); F. F. Abraham, *Phys. Rep.* **80**, 339 (1981).

²L. D. Landau and E. M. Lifshitz, *Statisticheskaya fizika*, Nauka, Moscow, 1976 (Statistical Physics, Pergamon Press, Oxford, 1980).

³A. Z. Patashinskii and V. L. Pokrovskii, *Fluktuatsionnaya teoriya fazovykh perekhodov* (Fluctuation Theory of Phase Transitions), Nauka, Moscow, 1982.

⁴V. L. Berezinskii, *Zh. Eksp. Teor. Fiz.* **59**, 907 (1970) [*Sov. Phys. JETP* **32**, 493 (1970)]; **61**, 1144 (1971) [*Sov. Phys. JETP* **34**, 610 (1971)].

⁵J. M. Kosterlitz and D. J. Thouless, *J. Phys. C* **6**, 1181 (1973).

⁶B. I. Halperin and D. R. Nelson, *Phys. Rev.* **B19**, 2457 (1979).

⁷A. P. Young, *Phys. Rev.* **B19**, 1855 (1979).

⁸V. L. Pokrovskii and A. L. Talapov, *Zh. Eksp. Teor. Fiz.* **78**, 269 (1980) [*Sov. Phys. JETP* **51**, 134 (1980)]; I. M. Khalatnikov (editor), *Soviet Science Reviews, Ser. Physics, Suppl. Vol. 1*, Harwood, New York, 1984.

⁹Yu. E. Lozovik and A. V. Klyuchnik, *Solid State Commun.* **37**, 335 (1980); *Solid State Commun.*, 1985 (in press).

¹⁰D. R. Nelson, *Phys. Rev.* **B27**, 2902 (1983).

¹¹Yu. E. Lozovik and V. M. Farztdinov, *Solid State Commun.* 1985 (in press).

¹²Y. Saito, *Phys. Rev. Lett.* **48**, 1114 (1982).

¹³A. N. Lagar'kov and V. M. Sergeev, *Usp. Fiz. Nauk* **125**, 409 (1978) [*Sov. Phys. Usp.* **21**, 566 (1978)].

¹⁴V. M. Bedanov, G. V. Gadiyak, and Yu. E. Lozovik, Preprint No. 31, Institute of Spectroscopy, Academy of Sciences of the USSR, Troitsk, 1985.

¹⁵R. W. Hockney, S. P. Goel, and J. W. Eastwood, *J. Comput. Phys.* **14**, 148 (1974).

¹⁶J. Q. Broughton, G. H. Gilmer, and J. D. Weeks, *Phys. Rev.* **B25**, 4651 (1982).

¹⁷C. C. Grimes and G. Adams, *Phys. Rev. Lett.* **42**, 795 (1979).

¹⁸D. A. Kirzhnits, *Usp. Fiz. Nauk* **119**, 357 (1976) [*Sov. Phys. Usp.* **19**, 530 (1976)]; O. V. Dolgov and E. G. Maksimov, *Usp. Fiz. Nauk* **135**, 441 (1981) [*Rev. Mod. Phys.* **53**, 81 (1981)].

¹⁹J. A. Barker, D. Henderson, and F. F. Abraham, *Physica (Utrecht)* **106A**, 226 (1981).

²⁰D. Frenkel and J. P. McTague, *Phys. Rev. Lett.* **42**, 1632 (1979).

²¹F. Van Swol, L. V. Woodcock, and J. N. Cape, *J. Chem. Phys.* **73**, 913 (1980).

²²S. Toxvaerd, *Phys. Rev.* **A24**, 2735 (1981).

²³J. P. McTague, D. Frankel, and M. P. Allen, in: *Ordering in Two Dimensions* (ed. S. K. Sinha), North-Holland, Amsterdam, 1980, p. 147.

²⁴R. W. Hockney and T. R. Brown, *J. Phys. C* **8**, 1813 (1975).

²⁵R. H. Morf, *Phys. Rev. Lett.* **43**, 931 (1979).

²⁶R. C. Gann, S. Chakravarty, and G. V. Chester, *Phys. Rev.* **B20**, 326 (1979).

²⁷R. K. Kalia and P. Vashishta, *Phys. Rev.* **B23**, 4794 (1981).

²⁸D. J. Thouless, *J. Phys. C* **11**, L189 (1978).

²⁹D. Fisher, *Phys. Rev.* **26**, 5009 (1982).

³⁰R. K. Kalia and P. Vashishta, *J. Phys. C* **14**, L643 (1981).

³¹A. T. Skjeltorp, *Phys. Rev. Lett.* **51**, 2306 (1983).

Translated by Dave Parsons